PROGRESS ON JAPANESE DEVELOPMENT OF ACCIDENT TOLERANT FeCrAl-ODS FUEL CLADDINGS FOR BWRS

K. SAKAMOTO, Y.MIURA
Nippon Nuclear Fuel Development, Co., Ltd.
2163 Narita-cho, Oarai-machi, Ibaraki-ken, 311-1313 – Japan

S. UKAI
Materials Science and Engineering, Faculty of Engineering, Hokkaido University
N13, W-8, Kita-ku, Sapporo, Hokkaido, 060-8628, Japan

A. KIMURA
Institute of Advanced Energy, Kyoto University
Gokasho, Uji, Kyoto 611-0011, Japan

A. YAMAJI
Waseda University
3-4-1, Okubo, Shinjuku-Ku, Tokyo, 169-8555, Japan

K. KUSAGAYA
Global Nuclear Fuel – Japan, Co., Ltd.
3-1, Uchikawa 2-Chome, Yokosuka-Shi, Kanagawa-Ken, 239-0836, Japan

T. KONDO
Hitachi-GE Nuclear Energy, Ltd.
1-1, Saiwai-cho, 3-chome, Hitachi-shi, Ibaraki-ken, 317-0073 Japan

S. YAMASHITA
Japan Atomic Energy Agency
2-4 Shirakata Shirane, Tokai-mura, Naka-gun, Ibaraki-ken 319-1195, Japan

ABSTRACT

This paper will introduce the progress of development of accident tolerant FeCrAl-ODS fuel claddings for BWRs (boiling water reactors) in the program sponsored and organized by the Ministry of Economy, Trade and Industry (METI) of Japan. In the development of FeCrAl-ODS fuel claddings both the experimental and the analytical studies have been performed. The experimental studies include the material irradiation tests in the ORNL High Flux Isotope Reactor (HFIR) and the simulated fuel rod irradiation tests. Both the experimental and the analytical studies in JFY2017 resulted in a successful step to develop the technical basis to introduce the FeCrAl-ODS fuel claddings in the current BWRs.

1. Introduction

A FeCrAl-ODS steel is a promising candidate alloy for the accident tolerant fuel cladding of LWRs (light water reactors) and being developed in Japanese projects recently [1] - [4]. This paper will introduce the progress of development of accident tolerant FeCrAl-ODS fuel claddings for BWRs (boiling water reactors) in the program sponsored and organized by the Ministry of Economy, Trade and Industry (METI) of Japan. In the development of FeCrAl-ODS fuel claddings both the experimental and the analytical studies have been performed. The experimental studies include the material irradiation tests in the ORNL High Flux Isotope Reactor (HFIR) and the simulated fuel rod irradiation tests. Basing on the progress in Japanese fiscal year (JFY) 2015 - 2016 [4] further multifaceted studies have

been promoted in JFY 2017. Key progresses in the experimental studies were expanding the database of mechanical properties of FeCrAl-ODS materials to the neutron irradiation of 2.6 dpa and some preliminary studies to examine the susceptibility to iodine SCC (I-SCC), wear, water quenching after steam oxidation at high temperatures and nitric acid solutions. In the analytical studies an applicability of FeCrAl-ODS fuel cladding to BWR MOX fuel was confirmed by a core analysis and a quantitative benefit was evaluated in the process of accident management. Moreover a steady preparation for the simulated fuel rod irradiation tests was conducted by analysis of fuel behavior and tests on welding and its inspection. This paper will cover mainly the experimental studies for normal operation and accident conditions. The result of tests to examine the effect of ion irradiation on corrosion property and the corrosion behavior in nitric acid solutions are separately presented in this meeting as Ref. 5 and Ref. 6, respectively. The details of core analysis will be given in the future meeting. The results of severe accident (SA) analysis [7], analysis of fuel behavior for the fuel irradiation tests [8] and the tests of welding and inspection [9], are presented in separate papers of this meeting.

2. Acquisition and accumulation of material properties

2.1 Materials fabrication

FeCrAl-ODS tube and FeCrAl rod materials were fabricated to support the evaluations in the analytical studies. Two types of tube materials were fabricated from master tubes. Both materials were fabricated by repeating cold-rolling and heat treatment.

One type of tube material was fabricated by four-pass cold rolling using conventional pilger mill to be the same outer diameter as the current 9x9 type A fuel cladding (11.2 mm) with about half wall-thickness (0.35 mm). The details are given in the previous paper [4]. In JFY2017 twelve rod materials were fabricated and the total length was over 16 m. Hereafter this type of tube material will be described as “9x9 type”.

Another type of tube material was fabricated to be the same wall thickness (0.35 mm) but smaller outer diameter as the current 10x10 type fuel cladding (10.3 mm). One rod material was fabricated with 1 m length. The first and the second cold-rollings were the same as the 9x9 type tube material (conventional pilger mill) but the third and the fourth one were conducted by three-rolling milling. Hereafter this type of tube material will be described as “10x10 type”.

2.2 Thermal properties

The coefficient of linear thermal expansion and melting point were measured by using the FeCrAl-ODS bar and sheet materials. The details of fabrication of bar and sheet materials were given in Ref. 4. Both measurements were performed by a thermomechanical analysis apparatus (NETZSCH, TMA4200SA).

In the thermal expansion measurement samples were heated up with a heating rate of 5 K/min up to 1673 K. Alumina was used as the standard material.

The melting point was measured by a thermal arrest method. The flakes of FeCrAl-ODS tube material were set inside of alumina holder and heated up with a heating rate of 6 K/min in an inert-gas atmosphere. The alumina holder was surrounded with a zirconium foil to maintain the oxygen potential to be sufficiently low. Gold and iron were used for the temperature calibration.

2.3 Mechanical properties

Uniaxial mechanical property of unirradiated and irradiated sheet material was obtained by a conventional tensile test. The schematic of specimens are shown in Fig. 1. The SS-J2 dog-bone tensile specimens were machined from the recrystallized sheet material. Two tensile directions were examined by using R-type and T-type specimens. The tensile direction of R-type specimen was parallel to the rolling direction of sheet material and that of T-type specimen was to the transverse direction. In some R-type specimens the welding bead with approximately 1 mm in width was introduced by an electron beam at the center of gauge section to examine the effect of welding on the mechanical properties. The neutron

irradiation was performed at High Flux Isotope Reactor (HFIR) in Oak Ridge National Laboratory (ORNL) at approximately 573 K. The estimated damage was approximately 2.6 dpa. The tensile test was conducted at a strain rate of 10^{-3} $s^{-1}$and temperatures of RT, 573 K and 623 K.

Biaxial mechanical property of unirradiated tube material was obtained by a conventional closed-end burst test. The tube material with 110 mm in length was set in the burst apparatus in NFD hot laboratory. The schematic of sample setting was shown in Fig. 2. Only two burst tests were performed as preliminary examinations at RT and 573 K to examine an applicability of existing method/apparatus for zirconium alloy materials to the FeCrAl-ODS tube materials.

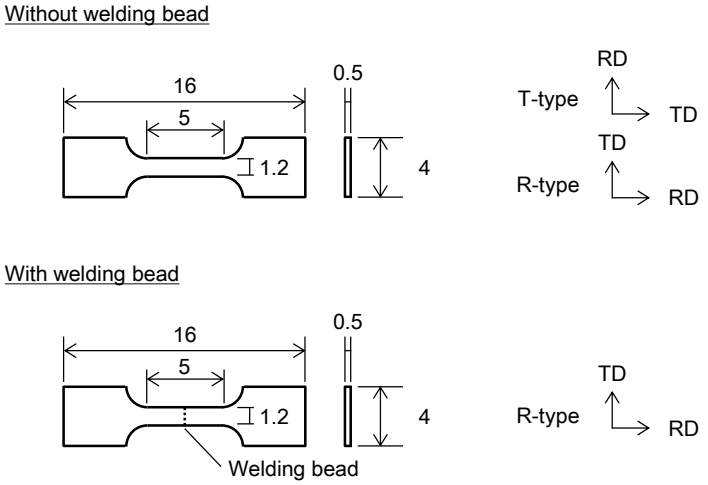

Fig. 1 Schematics of SS-J2 dog-bone specimens

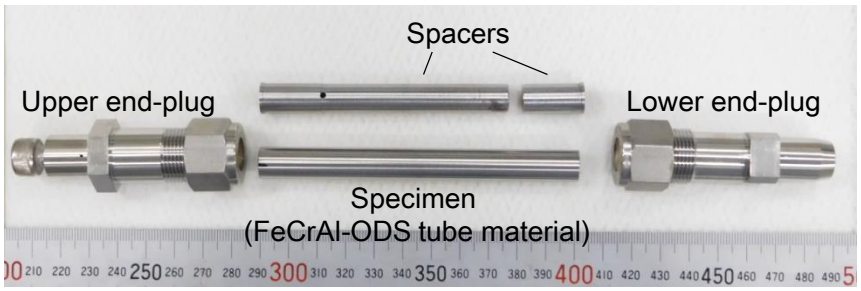

(a) Before assembly

(b) After assembly

Fig. 2 Overviews of specimen for closed-end burst test

2.4 Behaviors at normal operation condition

Some key material properties at normal operation condition were obtained.

Corrosion property of FeCrAl-ODS sheet and tube materials in BWR coolant was examined by the out-of-pile autoclave corrosion test. The conditions of corrosion test are the same as the previous study (563 K and 8 ppmDO. [Ref. 4]). The weight change was recorded up to approximately 150 d.

Iodine SCC (I-SCC) resistance of FeCrAl-ODS tube material was examined by introducing fresh iodine into inside of tube specimens with end-plugs. The cold-worked Zircaloy-2 tube

materials (without Zr-liner) were also subjected to the I-SCC. After the iodine introduction the specimens were maintained in an electric furnace at 523 K for 36 h to shorten the incubation time of I-SCC and the pinch load was applied at 623 K on the middle location of outer surface in the tube axial direction. The pinch load was generated by pushers with a displacement speed of 0.4 mm/h and the maximum displacement was approximately 1.5 mm for both materials.
Wear resistance of FeCrAl-ODS bar material was examined by a conventional sliding wear test under both dry and wet conditions. The Zircaloy-2 bar material was also subjected to the wear tests. SS304 bar material was selected as a counter material for both specimens. The micro-hardnesses of FeCrAl-ODS, Zircaloy-2 and SS304 bar materials were 345, 178 and 379 Hv, respectively. The contact force of 19.6 N was periodically applied by a reciprocal motion of the counter material with 10 Hz in 1.0 mm length.
Tritium permeability of FeCrAl-ODS bar material was evaluated by using the measuring system as reported in the previous study [Ref. 4]. The design of specimen was modified to reduce the leaking tritium from the disk edge by increasing the thickness of rim of the disk as shown in Fig. 3. The barrier effect of oxide layer formed in high temperature water was examined by using the specimen corroded in circulating hot water at 563 K and 8 ppm DO for 30 d. To simulate the configuration of oxide layer during the normal operation the oxide layer on one side was mechanically removed before the measurement. The steady-state permeability was measured for both the non- and corroded specimens with decreasing the specimen temperature. The non-steady-state permeation test was performed by using the corroded specimen by stepwise temperature increase of 50 K up to 573 K. The holding time at each temperature step was approximately 1 h up to 523 K and 24 h at 573 K.

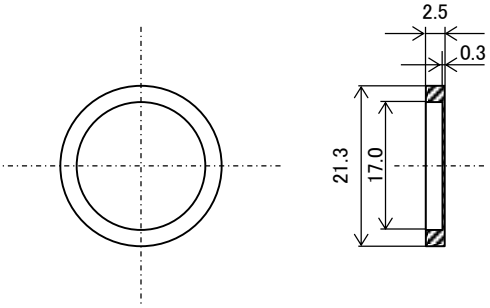

Fig. 3 Modified design of specimen for tritium permeation tests

2.5 Behaviors at accident conditions

The steam oxidation property of FeCrAl-ODS tube material was measured at 1473 – 1673 K. The ring-shaped specimens with 10 mm in length were suspended in the flow of wet Ar gas. The details of oxidation test were given in the previous paper [Ref. 4].
The resistance of FeCrAl-ODS tube material to water quenching after steam oxidation was examined by oxidizing the tube specimens (10 mm in length) at 1473 K in high temperature steam followed by water quenching. The oxidation time was 4, 8, 16 and 24 h and the temperature of water for quenching was maintained at 343 K. After the water quenching the ring specimens were subjected to the ring-compression test at RT to examine the change of mechanical properties by steam oxidation and water quenching. The maximum displacement was 8 mm (approximately 70 % of the diameter of specimen). The details of tests were given in Ref. 3.
The compatibility of FeCrAl-ODS sheet material with UO_2 pellet was examined below and above the melting point of FeCrAl-ODS materials. The tests below the melting point were performed at 1723 K (approximately 50 K below the melting point) for up to 25 h in an inert-gas atmosphere. As shown in Fig. 4, the reaction couple of FeCrAl-ODS sheet material and UO_2 pellet was set on alumina boat and contained inside of zirconium box to prevent the oxidation by residual oxidizing species in atmosphere. In the test above the melting point the reaction couple of FeCrAl-ODS sheet material and UO_2 pellet was heated up to 1853 K

(approximately 80 K above the melting point) in high temperature steam. The change of overview of specimen was recorded by a conventional video camera as shown in Fig. 5. The former test is attributed to the condition of fuel cladding and fuel pellet without burst opening during accident conditions. The later one is to simulate the condition at severe accident with exposure of fuel cladding and fuel pellet to high temperature steam.

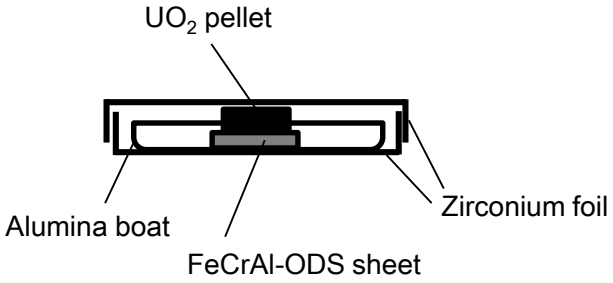

Fig. 4 Experimental set-up of specimen for compatibility test below melting point

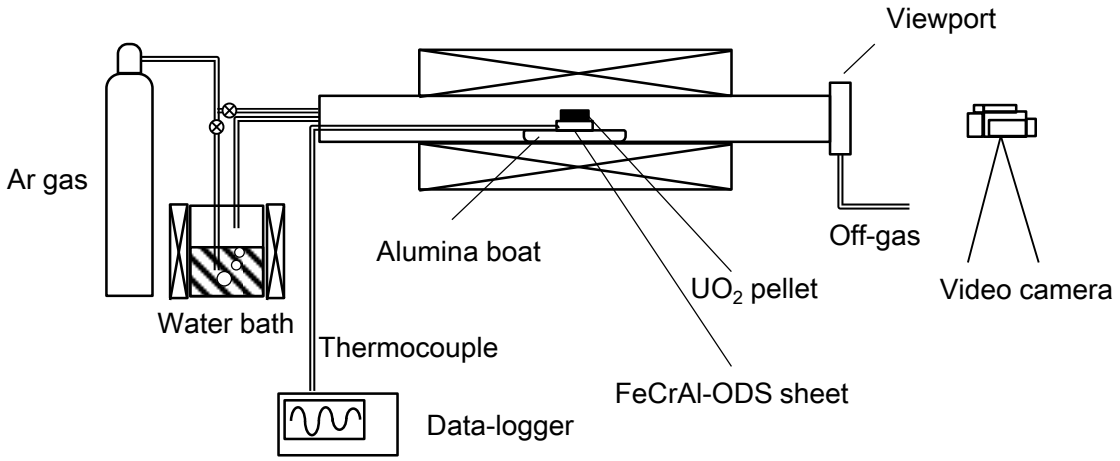

Fig. 5 Experimental set-up of measuring system for compatibility test above melting point

3. Results and Discussion

3.1 Materials fabrication

The overview of twelve 9x9 type FeCrAl-ODS tube materials is shown in Fig. 6. Since small samples were taken at each cold-rolling and heat-treatment steps for metallurgical observations and micro-hardness measurements, one tube was shorter than other 11 tubes. The distributions of diameter and thickness along the tube axial direction were measured at both ends of sectioned pieces of five tubes. As can be seen in Fig. 7 the axial distributions of diameters and thicknesses were uniform and almost the same among five tube materials. The overview of one 10x10 type FeCrAl-ODS tube material is shown in Fig. 8. The axial distributions of diameter and thickness are plotted in Fig. 9. A similar uniform distribution was also found in the 10x10 type FeCrAl-ODS tube material whereas a further accumulation is clearly needed to confirm the productivity of tube fabrication by the three-roll milling.

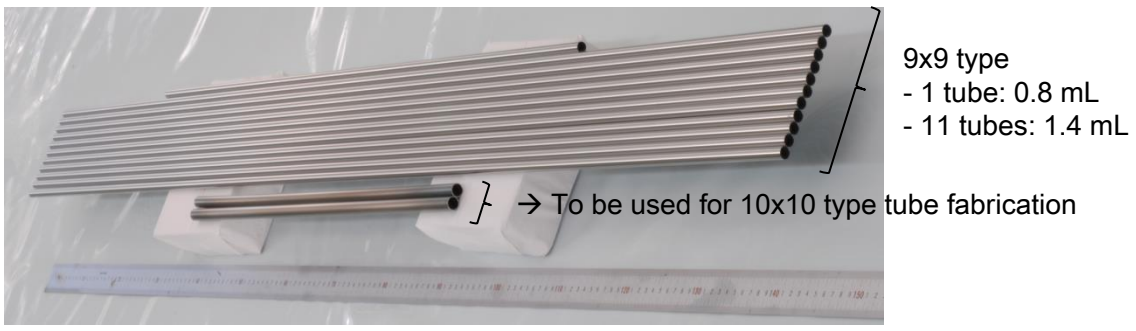

Fig. 6 Overview of fabricated 9x9 type FeCrAl-ODS tube materials

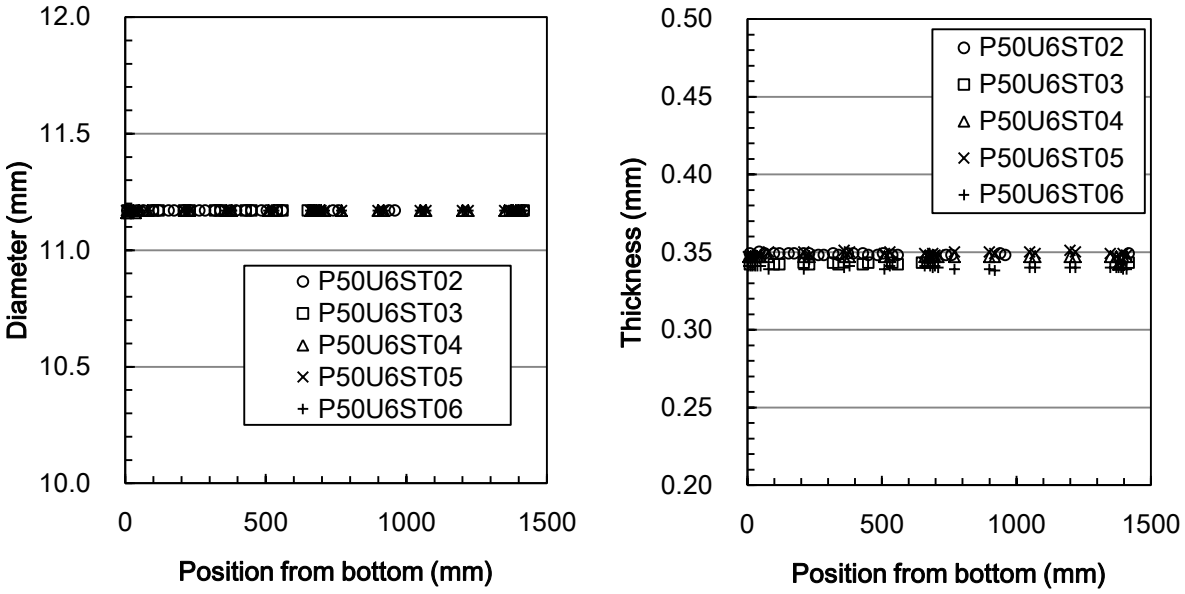

(a) Diameter (b) Thickness

Fig. 7 Axial distributions of diameters and thicknesses of 9x9 type FeCrAl-ODS tube materials

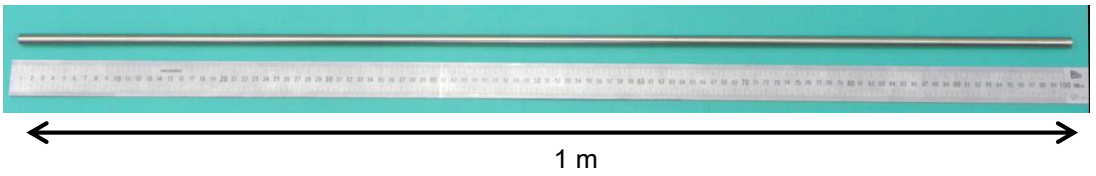

Fig. 8 Overview of fabricated 10x10 type FeCrAl-ODS tube material

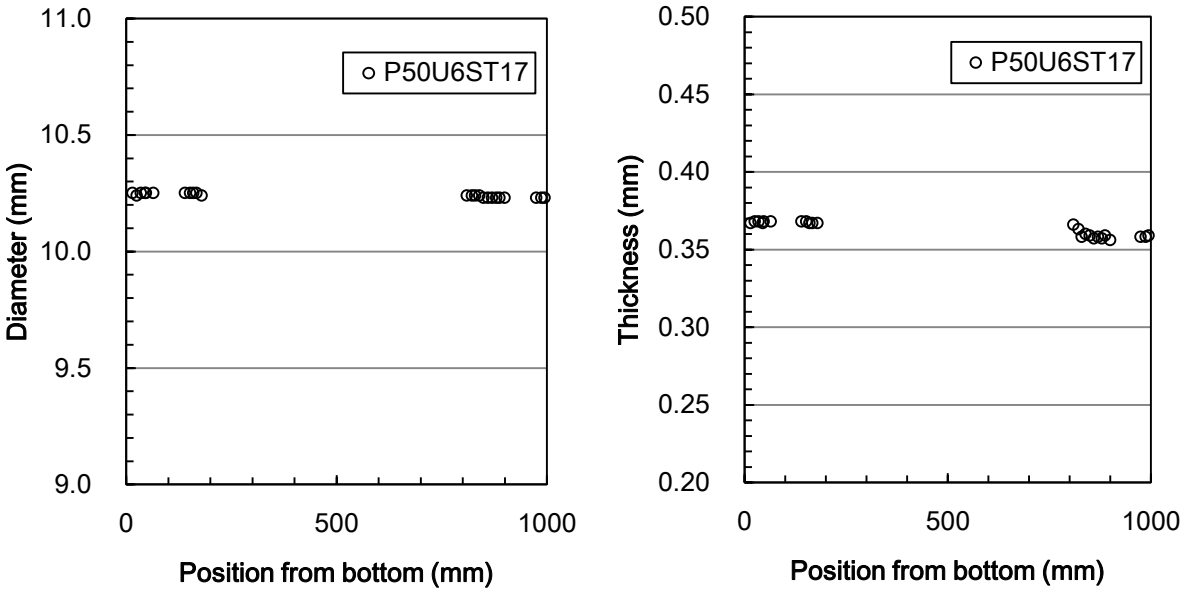

Fig. 9 Axial distributions of diameter and thickness of 10x10 type FeCrAl-ODS tube material

3.2 Thermal properties

No significant difference was found among three types of samples; rolling and transverse direction of sheet material and bar material. The averaged coefficient of linear thermal expansion α of the FeCrAl-ODS material was given by the following equation.

$$\alpha = -3.383 \times 10^{-12} T_c^4 + 1.098 \times 10^{-8} T_c^3 - 1.150 \times 10^{-5} T_c^2 + 8.270 \times 10^{-3} T_c + 1.081 \times 10^{1}. \qquad 50\,℃ \leq T_c \leq 1400\,℃$$

Here T_c is temperature in ℃. The temperature dependence of α was compared with FeCrAl and Zircaloy materials in Fig. 10. The α of FeCrAl-ODS was in good agreement with that of FeCrAl [10] and approximately double of that of Zircaloy [11]. From the viewpoint of fuel behavior analysis this difference of thermal expansion should be taken into account.
The melting point was measured three times and the evaluated melting point T_m of FeCrAl-ODS was given as the following.

$T_m = 1503 \pm 1.5$℃

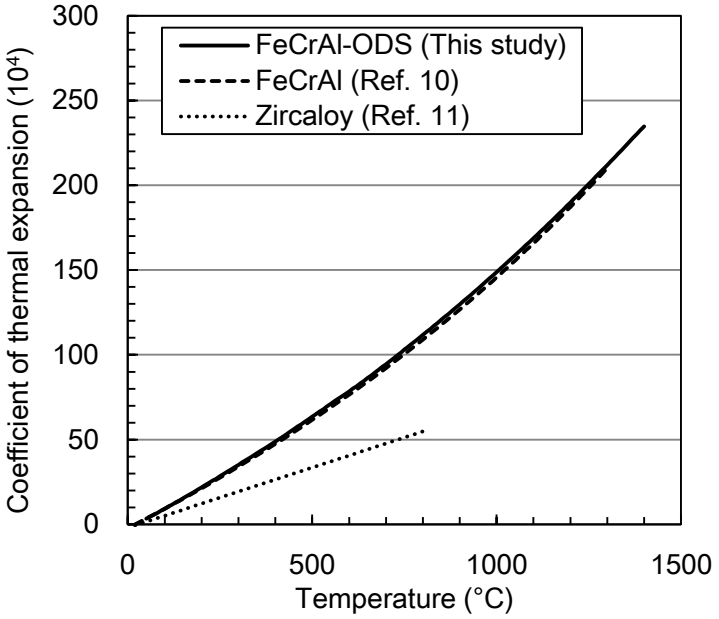

Fig. 10 Temperature dependence of α

3.3 Mechanical properties

In Fig. 11 the temperature dependence of strength of recrystallized FeCrAl-ODS sheet materials are compared between unirradiated and irradiated specimens. All data were obtained by the uniaxial tensile tests. The irradiation hardening by neutron irradiation of 2.6 dpa was confirmed in both ultimate tensile and yield stresses. The hardening was more pronounced in the yield stress since strain hardening was less significant in the irradiated specimens. The isotropic manner was also confirmed by comparing the T-type (transverse direction) and R-type (rolling direction). Since the transverse and rolling directions of sheet material are respectively attributed to the axial and hoop directions of tube material, the recrystallized FeCrAl-ODS tube material would be regarded as an isotropic material in fuel behavior analyses. No significant decrease of strength was found in the specimens with welding bead.
The closed-end burst tests were successfully performed in both temperatures (RT and 573 K). The hoop stress – hoop strain relationship obtained in the test at 573 K is shown in Fig. 12. It should be noted that the maximum hoop strain in the figure does not represent the value in the whole specimen since the measuring elevation of diameter was not the same as that of burst opening (~ maximum deformed area). The overview of specimen after the burst in the test at 573 K is shown in Fig. 13. Further measurements will be done to accumulate the data on biaxial tensile property.

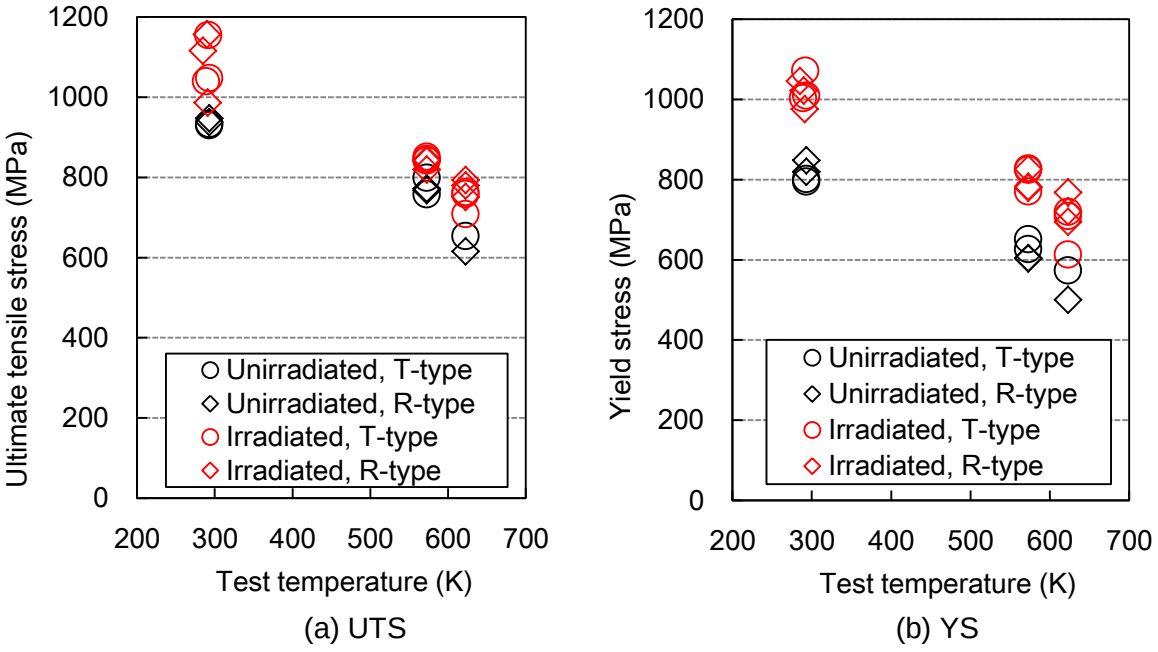

Fig. 11 Temperature dependence of strength of FeCrAl-ODS sheet materials

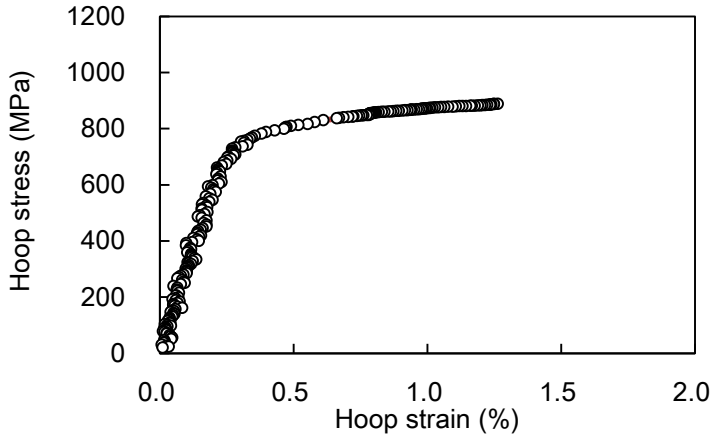

Fig. 12 Hoop stress – hoop strain relationship obtained in closed-end burst test at 573 K

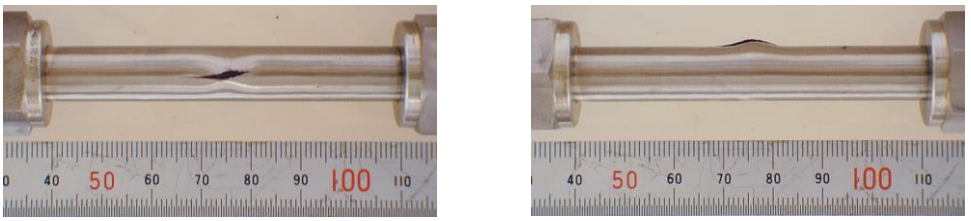

Fig. 13 Overview of specimen after closed-end burst test at 573 K

3.4 Behaviors at normal operation condition

The weight changes of FeCrAl-ODS and reference materials are summarized in Fig. 14. Both FeCrAl-ODS materials maintained a good corrosion resistance in the range examined in the present study.

Three I-SCC tests were conducted for each material in the same experimental conditions

and contrasting results were obtained between FeCrAl-ODS and Zircaloy-2 tube materials. Long axial cracks were found inside of Zircaloy-2 tube materials beneath the contacted locations with the pusher whereas no crack initiation was confirmed in FeCrAl-ODS tube materials (Fig. 15). To compare the conditions of cracking local plastic strains were estimated at the locations where the axial cracks were found in Zircaloy-2 tube materials since the diameters and wall-thicknesses were different each material. The maximum local plastic strains in Zircaloy-2 and FeCrAl-ODS tube materials were respectively estimated to be 0.013 – 0.017 and 0.006 - 0.010. The tentative conclusion was that the FeCrAl-ODS has a good resistance to I-SCC but further I-SCC tests are clearly needed for FeCrAl-ODS tube material to cover the range of local plastic strain to make a direct comparison with Zircaloy-2 material.

An example of outer surfaces of FeCrAl-ODS and Zircaloy-2 bar materials after the sliding wear tests is shown in Fig. 16. After the sliding wear tests in water for 90 min with 10 Hz a slight trace of wear was found in FeCrAl-ODS bar material whereas a wider and deeper wear traces was formed on Zircaloy-2 bar material. The wear depths measured after the sliding wear tests are summarized in Fig. 17. The wear depth of FeCrAl-ODS bar material was much smaller than that of Zircaloy-2 bar material in both the dry and wet conditions. In the wet sliding wear tests the wear depth of FeCrAl-ODS bar material remained to be small whereas that of Zircaloy-2 bar material became more significant with time. As far as the range examined in the present study the FeCrAl-ODS materials can be expected to have a good resistance to sliding wear. This good resistance would be owing to high strength and high hardness. A further test will be performed to examine the influence of loading mode such as impact loading.

In the tritium permeation tests of non-corroded specimens a better linearity was obtained in the temperature dependence (Arrhenius plot) as shown in Fig. 18. This good linearity would be attributed to the modification of sample design. In the tritium permeation testes of corroded specimens a weak barrier effect was found and the permeation reduction factors (PRF) were in the range of 2.5 – 3.9. This weak barrier effect was inconsistent with the previous study [4] where the tritium permeation was suppressed significantly by the oxide layer. The main reason of this contradictory would be an insufficient time to measure the steady-state permeability in the previous study. The holding time should be needed longer in the previous study since the thickness of disk sample was thicker (0.5 mm) than that in this study (0.3 mm) and, moreover, the tritium permeability was measured with increasing temperature. According to the comparison between the previous and the present tests the non-steady-state test was conducted to examine the limit of barrier effect of oxide layer with increasing the sample temperature. In Fig. 19 the tritium permeability of corroded FeCrAl-ODS bar material was shown as a function of the time after the tritium gas exposure. No measurable tritium permeation was found in the increasing steps from RT to 573 K. A significant tritium permeation was shown approximately 2 h after the holding at 573 K. Further tests will be performed to examine the healing effect of steam or water on the oxide layer at high temperatures.

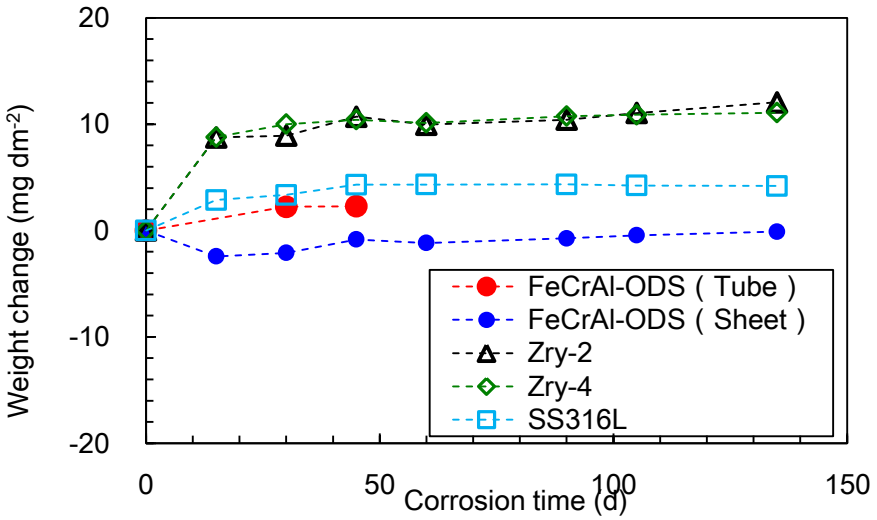

Fig. 14 Weight changes of FeCrAl-ODS and reference materials in high temperature water at 563 K and 8 ppmDO

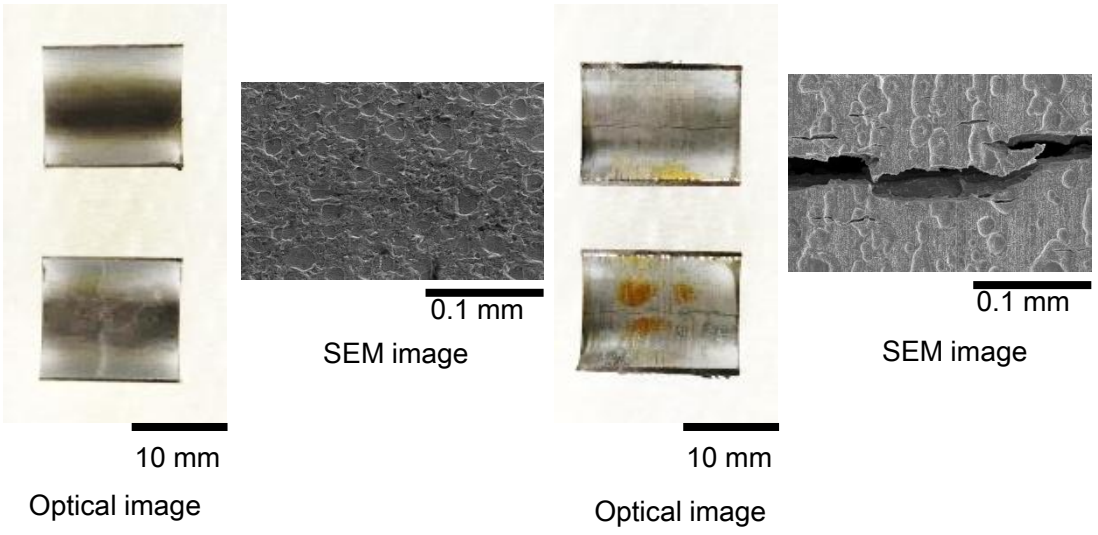

(a) FeCrAl-ODS tube

(b) CW Zircaloy-2 tube (without Zr-liner)

Fig. 15 Inner surfaces of FeCrAl-ODS and CW Zircaloy-2 tubes after I-SCC tests

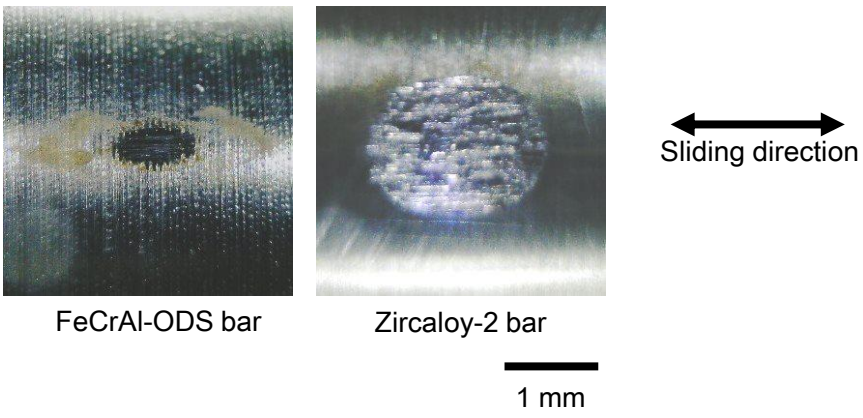

Fig. 16 Outer surfaces of FeCrAl-ODS and Zircaloy-2 bar materials after sliding wear tests (90 min in water)

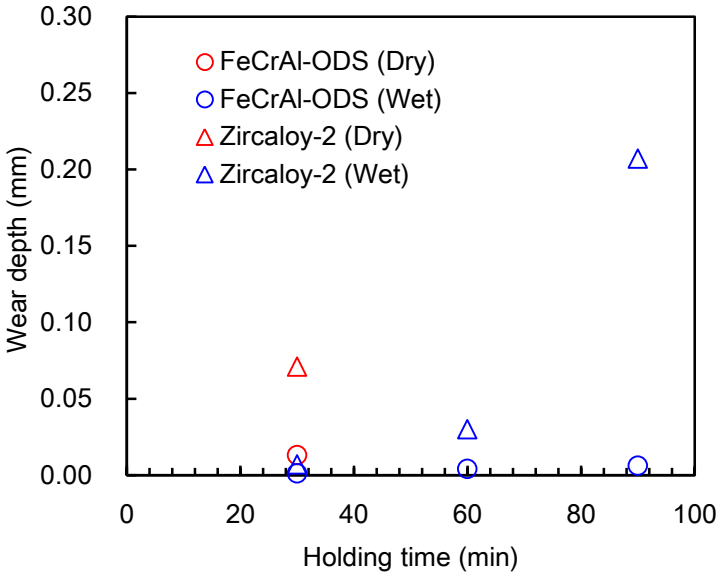

Fig. 17 Wear depth of FeCrAl-ODS and Zircaloy-2 bar materials after sliding wear tests

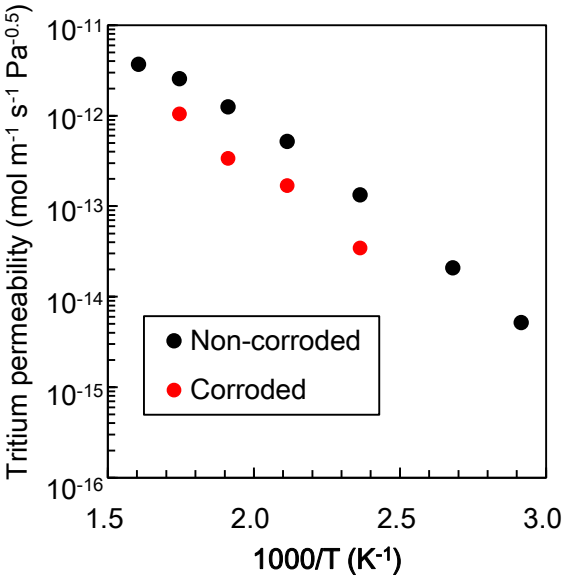

Fig. 18 Temperature dependence of steady-state tritium permeability of FeCrAl-ODS rod materials with and without oxide layer

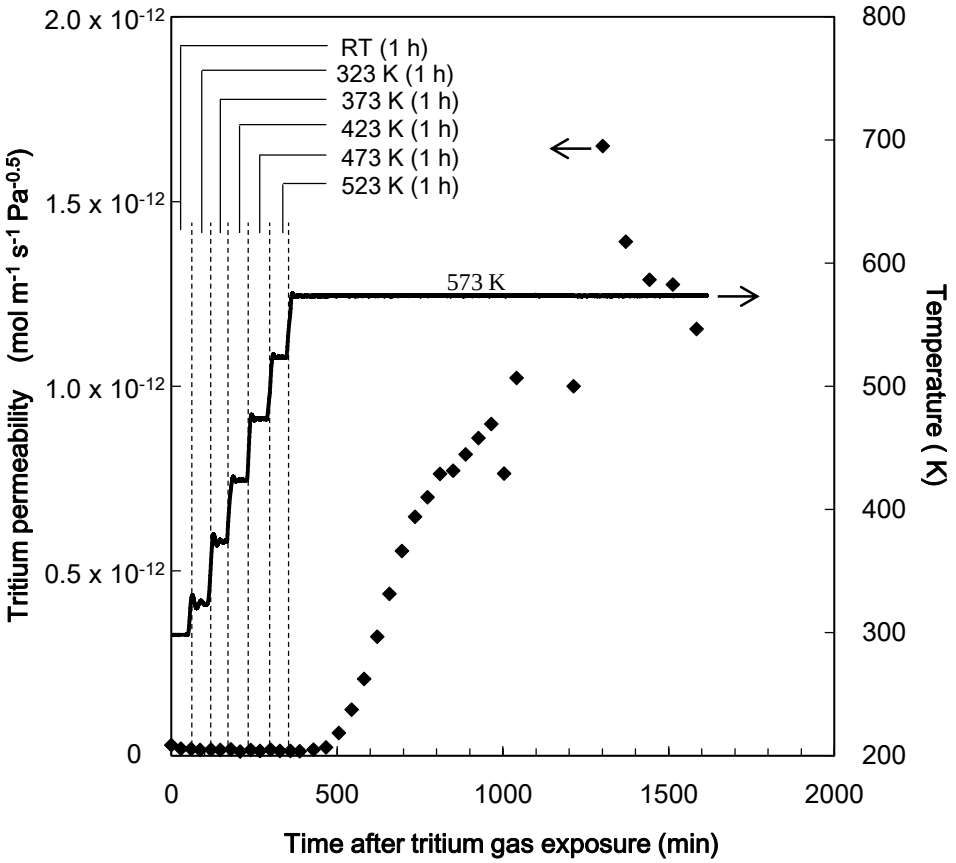

Fig. 19 Tritium permeation through corroded FeCrAl-ODS rod material in non-steady-state permeation test

3.5 Behaviors at accident condition

The value of the reaction rate constant K_p of FeCrAl-ODS materials obtained in this study was compared with other materials in Fig. 20. Here the weight gain (WG) is a function of time *t* as $WG = K_p t^{0.5}$. The difference of K_p among FeCrAl-ODS materials was small and the value was comparable to APMT (FeCrAl alloy) [14] and smaller by 2 – 3 orders compared to Zry-4 [12] and SS304 [13]. This result implies that the microstructure and shape of FeCrAl-ODS material has no or slight effect on the steam oxidation property and the resistance to high temperature steam is superior to the current material regardless of its microstructure and shape.

No apparent cracks and failures were observed after the water quenching in the tests to examine the resistivity of FeCrAl-ODS tube materials to water quenching after steam oxidation at 1473 K for up to 24 h. The results of ring compression tests after water quenching are summarized in Fig. 21 where the normalized load was calculated by dividing the applied load by the specimen length. The specimen without steam oxidation (0 h) resulted in cracking over the displacement of 6 mm whereas no cracking was found in all specimens with steam oxidation at 1473 K for 4 – 24 h. This result demonstrated a high resistivity of FeCrAl-ODS tube materials in both steam oxidation at high temperatures and thermal shock. The reason of enhanced elongation by steam oxidation is not clear whereas a softening would proceed during the holding time at high temperatures.

The compatibility tests with UO_2 pellet were conducted at 1723 K for 4, 9 and 25 h in an inert-gas atmosphere. The cross-sectional observation was performed at the center of contact area. By the SEM-EDS analysis no cross-diffusion between FeCrAl-ODS sheet material and UO_2 pellet was observed but Al-oxide layer was formed at the interface. Fig. 22 shows the results of optical observation and the SEM-EDS analysis at the interface of specimen maintained at 1723 K for 25 h. The Al-oxide layer with 4 μm thickness played a

role of a barrier for the reaction. The average growth rate of Al-oxide layer decreased with the holding time; 6.3 x 10^{-12} cm^2 s^{-1} was for 4 h, 2.3 x 10^{-12} cm^2 s^{-1} for 9 h and 1.4 x 10^{-12} cm^2 s^{-1} for 25 h. This trend would suggest that the diffusions of Al and O were suppressed with the thickness of Al-oxide layer. The growth rates obtained in this study were comparable to those measured with a shorter holding time (1 h) at 1573 – 1723 K in the previous study [4] and smaller by 5 – 6 orders compared to the growth rates of reaction layer between Zircaloy and UO_2 pellet (10^{-5} – 10^{-6} cm^2 s^{-1}) [15]. The compatibility test in high temperature steam was conducted with increasing temperature up to 1853 K. The overviews of specimens before and after the compatibility test were shown in Fig. 23. No significant change was found in the shape of UO_2 pellet whereas the FeCrAl-ODS sheet materials did not retain its original shape. According to the video record during the test no detectable change was observed up to approximately 1800 K but above the temperature the FeCrAl-ODS sheet material changed its shape in a short time. To confirm the reaction between the UO_2 pellet and ex-FeCrAl-ODS sheet the cross-sectional observation and analysis was performed as shown in Fig. 24. A clear ingress of FeCrAl-ODS elements into UO_2 pellet was observed in area 1 where the UO_2 pellet was covered with the ex-FeCrAl-ODS sheet. On the other hand no change was found in area 2 in the optical image where no direct contact would be generated between UO_2 pellet and ex-FeCrAl-ODS sheet. An understanding of the details of reaction needs a further analysis while the Al-oxide layer would not be able to play a role of barrier with a significant change in shape and oxidation state by a rapid oxidation of FeCrAl-ODS material.

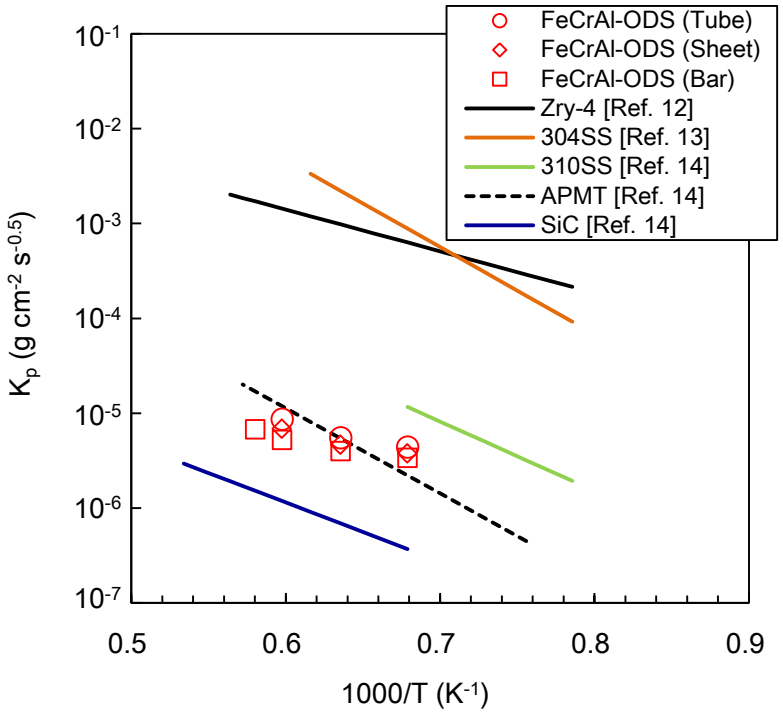

Fig. 20 Temperature dependence of K_p of FeCrAl-ODS materials

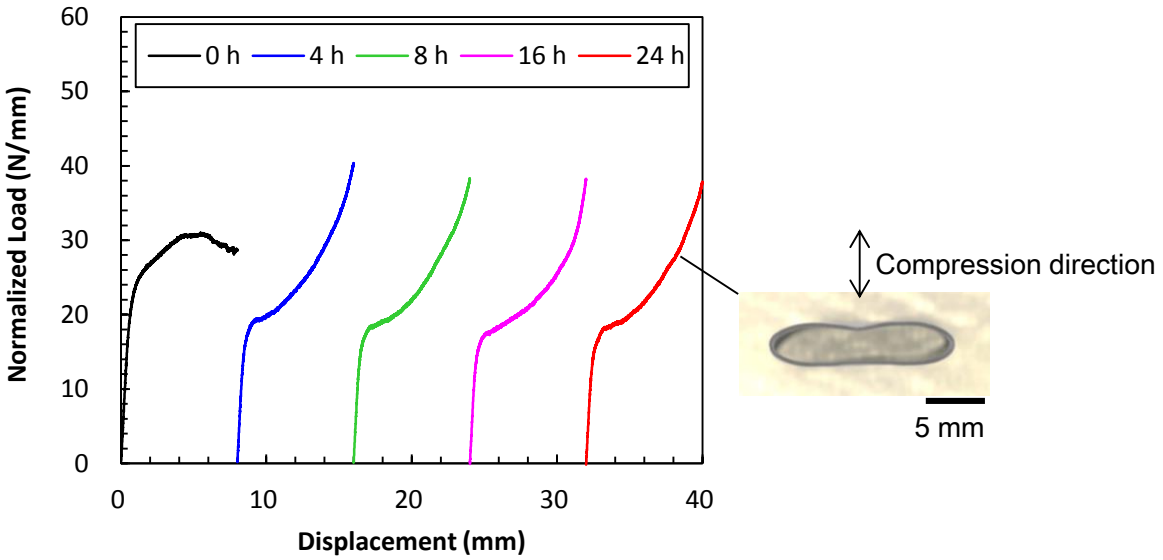

Fig. 21 Load – displacement curves of FeCrAl-ODS tube materials after steam oxidation and water quenching

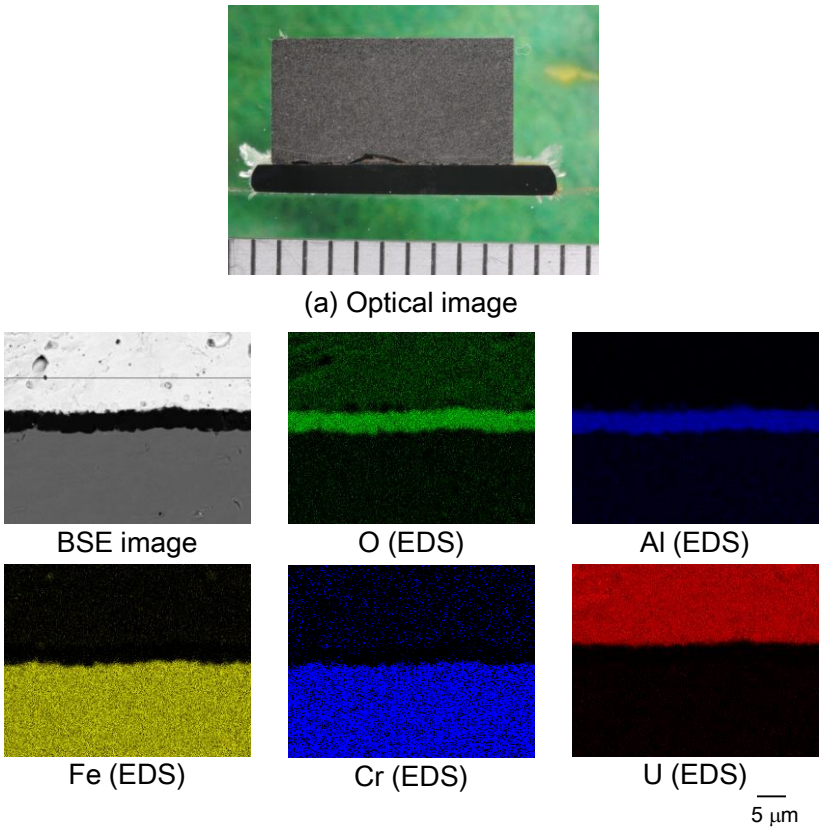

Fig. 22 Result of SEM-EDS analysis of cross-section of contact area after compatibility test at 1723 K for 25 h

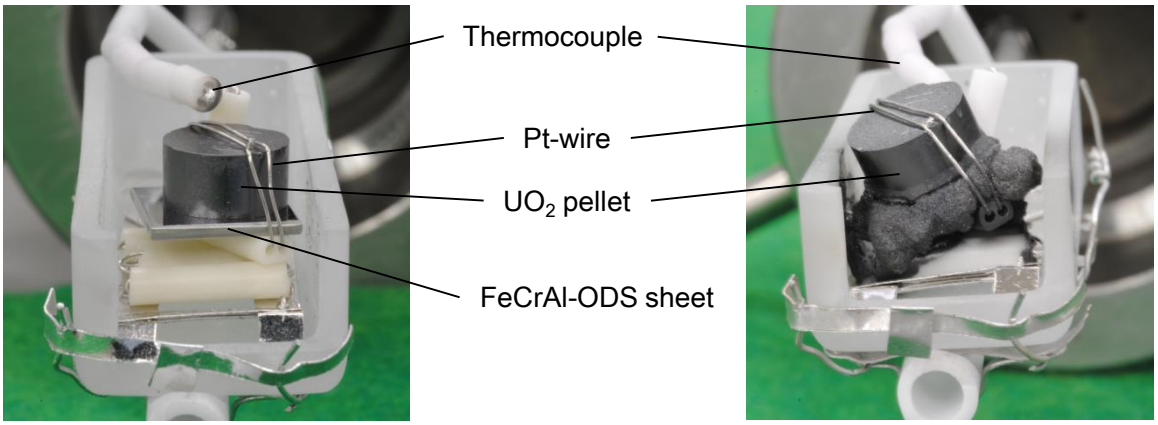

Fig. 23 Overviews of specimens before and after compatibility tests in high temperature steam up to 1853 K.

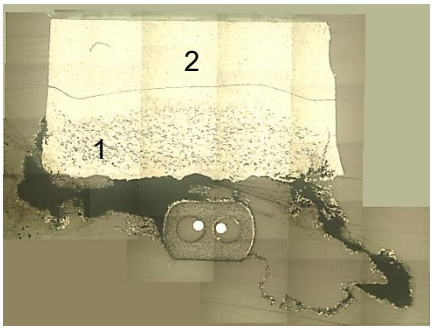

(a) Optical image

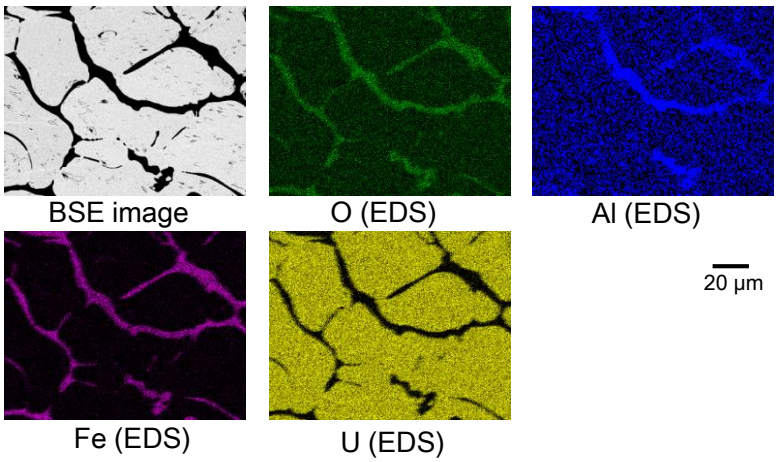

(b) SEM-EDS analysis of center part of area 1

Fig. 24 Result of SEM-EDS analysis of cross-section of specimen after compatibility tests in high temperature steam up to 1853 K

4. Conclusion

Basing on the progress in 2015 - 2016 further multifaceted studies have been promoted in JFY 2017 on the development of accident tolerant FeCrAl-ODS fuel claddings for BWRs in the program sponsored and organized by the Ministry of Economy, Trade and Industry (METI) of Japan. Both the experimental and the analytical studies in JFY2017 resulted in a successful step to develop the technical basis to introduce the FeCrAl-ODS fuel claddings in the current BWRs.

5. References

[1] S. Ukai, N. Oono, S. Ohtsuka, T. Kaito, K. Sakamoto, T. Torimaru, A. Kimura, S. Hayashi, "Development of FeCrAl-ODS steels for ATF cladding", Proceedings of Top Fuel 2016, Boise, ID, Sep. 11-15 (2016) 681-689.

[2] S. Ukai, N. Oono, K. Sakamoto, T. Torimaru, T. Kaito, A. Kimura, S. Hayashi, "Development of FeCrAl-ODS steel claddings for accident tolerant fuel of light water reactors", Proceedings of ICAPP 2017, Fukui and Kyoto, Japan, April 24-28 (2017) Paper ID: 17599.

[3] K. Sakamoto, T. Torimaru, S. Ukai, N. Oono, T. Kaito, A. Kimura, S. Hayashi, "Preliminary performance evaluation of FeCrAl-ODS steel fuel cladding under accident conditions of BWRs", Proceedings of ICAPP 2017, Fukui and Kyoto, Japan, April 24-28 (2017) Paper ID: 17707.

[4] K. Sakamoto, M. Hirai, S. Ukai, A. Kimura, A. Yamaji, K. Kusagaya, T. Kondo, S. Yamashita, "Overview of Japanese development of accident tolerant FeCrAl-ODS fuel claddings for BWRs", Proceedings of 2017 Water Reactor Fuel Performance Meeting, Ramada Plaza Jeju, Jeju Island, Korea, Sep. 10-14 (2017) Paper ID: A-033.

[5] T. Sato, Y. Nakahara, F. Ueno, K. Sakamoto, S. Yamashita, " Effect of ion irradiation on the corrosion of FeCrAl-ODS in high temperature water simulating BWR conditions", to be published in Proceedings of Top Fuel 2018.

[6] Y. Takahatake, H. Ambai, Y. Sato, M. Takeuchi, K. Koizumi, K. Sakamoto, S. Yamashita, "Corrosion behavior of FeCrAl-ODS steels in nitric acid solutions at several temperatures", to be published in Proceedings of Top Fuel 2018.

[7] T. Ikegawa, T. Kondo, K. Sakamoto, S. Yamashita, "Performance evaluation of accident tolerant fuel claddings during severe accidents of BWRs", to be published in Proceedings of Top Fuel 2018.

[8] N. Susuki, A. Yamaji, K. Kusagaya, K. Sakamoto, S. Yamashita, "Analysis of irradiation matrix for the Japanese FeCrAl-ODS test fuel rods irradiations at the Halden Reactor using FEMAXI-7 code ", to be published in Proceedings of Top Fuel 2018.

[9] A. Kimura, S. Yuzawa, K. Sakamoto, M. Hirai, S. Ukai, A. Yamaji, K. Kusagaya, T. Kondo, S. Yamashita, " Welding Technology R&D of Japanese Accident Tolerant FeCrAl-ODS fuel claddings for BWRs (2)", to be published in Proceedings of Top Fuel 2018.

[10] K. G. Field, M. A. Snead, Y. Yamamoto, K. A. Terrani, “Handbook on the material properties of FeCrAl alloys for nuclear power production applications”, ORNL/TM-2017/186 Rev.0, August 2017.

[11] D. L. Hagrman, G. A. Reymann, R. E. Mason, “MATPRO-Version 11 (Revision 2): A hand book of materials properties for use in the analysis of light water reactor fuel rod behavior”, NUREG/CR-0497 (TREE-1280, Rev. 2, R3 and R4), August 1981.

[12] J.V. Cathcart, R.E. Pawel, R.A. McKee, R.E. Druschel, G.J. Yurek, J.J. Campbell, S.H. Jury, “Zirconium Metal–Water Oxidation Kinetics”, IV: Reaction Rate Studies, ORNL/NUREG-17, Oak Ridge National Laboratory, 1977.

[13] T. Ishida, Y. Harayama, S. Yaguchi, “Oxidation of 304 stainless steel in high-temperature steam”, J. Nucl. Mater., 140 (1986) 74-84.

[14] B.A. Pint, K.A. Terrani, M.P. Brady, T. Cheng, J.R. Keiser, “High temperature oxidation of fuel cladding candidate materials in steam–hydrogen environments”, J. Nucl. Mater., 440 (2013) 420–427.

[15] P. Hofmann, “Current knowledge on core degradation phenomena, A review,” J. Nucl. Mater., 270, 1-2, 194-211 (1999).

Acknowledgement
This study is the result of “Development of Technical Basis for Introducing Advanced Fuels Contributing to Safety Improvement of Current Light Water Reactors” carried out under the Project on Development of Technical Basis for Improving Nuclear Safety by Ministry of Economy, Trade and Industry (METI) of Japan.